

# Complex light with optical singularities induced by nanocomposites

Vlad V. Ponevchinsky and Marat S. Soskin\*

*Institute of Physics, NAS of Ukraine, 46 Prospect Nauki, Kyiv 03650, Ukraine*

Andrei I. Goncharuk and Nikolai I. Lebovka†

*Institute of Biocolloidal Chemistry named after F. Ovcharenko,  
NAS of Ukraine, 42 Vernadskii Prosp., Kyiv 03142,  
Ukraine, Tel. +380-44-424-03-78, Fax: +380-44-424-80-78*

Sergei V. Naydenov and Longin N. Lisetski

*Institute for Scintillation Materials of STC "Institute for Single Crystals" of the National Academy of Sciences of Ukraine,  
60 Lenin Ave., 61001 Kharkov, Ukraine, Tel. +380-57-341-03-58, Fax: +380-57-758-69-18*

(Dated: January 6, 2011)

The nanocomposites on the base of long (5-10  $\mu\text{m}$ , *o*-MWCNTs) and short (2  $\mu\text{m}$ , *m*-MWCNTs) multi-walled carbon nanotubes (MWCNTs) hosted by nematic 5CB were investigated in details by means of polarizing microscopy, studies of electrical conductivity and electro-optical behaviour. The spontaneous self-organization of MWCNTs was observed and investigated both theoretically and experimentally. The efficiency of MWCNT aggregation in these composites is controlled by strong, long ranged and highly anisotropic van der Waals interactions, Brownian motion of individual nanotubes and their aggregates. The simple Smoluchowski approach was used for estimation of the half-time of aggregation. It was shown that aggregation process includes two different stages: fast, resulting in formation of loose aggregates (*L*-aggregates) and slow, resulting in formation of compacted aggregates (*C*-aggregates). Both *L*- and *C*-aggregates possess extremely ramified fractal borders. Formation of the percolation structures was observed for *o*-MWCNTs at  $C = C_p \approx 0.0025$ -0.05 % wt and for *m*-MWCNTs at  $C = C_p \approx 0.005$ -0.25 % wt. A physical model describing formation of *C*-aggregates with captured 5CB molecules inside was proposed. It shows good agreement with experimentally measured characteristics. It was shown that MWCNTs strongly affect the structural organization of LC molecules captured inside the MWCNT skeleton and of interfacial LC layers in the vicinity of aggregate borders. Moreover, the structure of the interfacial layer, as well as its birefringence, drastically changed when the applied electric voltage exceeded the Fredericksz threshold. Finally, formation of the inversion walls between branches of the neighbouring MWCNT aggregates was observed and discussed for the first time.

PACS numbers: 02.40.-k, 42.25.Ja, 42.30.Ms, 61.30.-v, 61.46.-w, 73.63.Fg, 73.22.-f

## I. INTRODUCTION AND MOTIVATION OF THE PROBLEM

Complex light is an essential chapter of the modern optics. It is especially actual for the light fields containing optical singularities and special topological structures. Nanoscience and nanotechnology are the hot spots now. Many promising composites on the base of nanoparticles incorporated into continuous macro host were recently proposed. The classical examples are colloidal dispersions of nanoparticles in liquid crystals (LC) [1, 2]. Typically, concentration of nanofiller in a LC host is rather small, which allows preserving the principal properties of the host [3]. However, in many cases self-organisation of nanofiller inside LC host provokes appearance of unusual nanostructures with essentially new and nontrivial properties. Note that perturbation of uniaxial nematic LC may result in birth of additional topological structures

up to singularities [3]. These effects may be especially strong in nematics filled by nanoparticles. It was recently demonstrated that propagation of laser beam through the uniaxial nematic 5CB filled with multi-walled carbon nanotubes (MWCNTs) generated the complex light and nano-particles originated spontaneous birth of optical singularities in a LC host [4,5].

The interesting data on the optical, electrophysical, and thermodynamic properties of nematic 5CB filled with MWCNTs were already reported [6-8]. Irreversible self-organisation of MWCNTs results in formation of fractal aggregates [9] with extremely ramified fractal borders [6,7]. An individual aggregate consists of MWCNT skeleton with captured 5CB molecules inside. Moreover, each aggregate perturbs the micron-sized interfacial LC layers producing the random director orientations in the vicinity of the aggregate. The hexagon dimensions in 5CB molecule match excellently the hexagon structure of MWCNT [2] and theory [10] predicts that 5CB molecules can be extra strongly anchored to the side walls of nanotubes. The energy of interaction between 5CB and surface of nanotubes is of the order of -2eV that is two orders of magnitude higher than the thermal energy  $kT$ .

\*Electronic address: marat.soskin@gmail.com

†Electronic address: lebovka@gmail.com

Such strong interactions may define unique optical and other physical characteristics of the 5CB + MWCNT composite called legally "scientific duo" [2]. Moreover, self-organisation and aggregation of the particles with highly anisotropic shape in anisotropic fluids is still far from full understanding and requires thorough theoretical and fundamental studies [11].

The main aim of the present investigations was the study of aggregation, electrical conductivity and electrooptical effects in 5CB filled by MWCNTs. The work discusses effects of spontaneous self-aggregation and percolation, theoretical model of fractal aggregation, capturing of LC molecules inside MWCNT skeleton and interfacial LC layers in the vicinity of aggregates, electrooptical data and electric field induced formation of inversion walls.

## II. MATERIALS AND EXPERIMENTAL TECHNIQUES

### A. Liquid crystal

5CB (4-pentyl-4'-cyanobiphenyl) was used as a nematic host. It was obtained from Chemical Reagents Plant, Kharkov, Ukraine. The pure 5CB demonstrates the presence of a weakly first order isotropic to nematic transition at  $T_{ni} \approx 308 - 309$  K and a strongly first order nematic to crystal transition at  $T_{cn} = 295.5$  K.

### B. Multiwalled carbon nanotubes

The MWCNT preparation procedure is described in detail in [6]. It is known that all the properties of carbon nanotubes depend strongly on their aspect ratio [1, 2]. Two types of powdered MWCNTs were investigated: (i) "long" *o*-MWCNTs with  $5 \div 10 \mu\text{m}$  length (ii) and "short" *m*-MWCNTs with  $\approx 2 \mu\text{m}$  length obtained by careful grinding of long MWCNTs in a mill. The MWCNT aspect ratio was  $\approx 500$  and  $\approx 200$  for long and short CNTs, respectively.

### C. Preparation of MWCNT+5CB composites

Before sonication, MWCNTs form dense blocks sized up to  $50 \mu\text{m}$ , which consist of nanotube bundles (tangles) [6]. Their mixture with chemically pure 5CB was ultrasonicated (20 min) carefully up using a UZDN-2T ultrasonic disperser to the apparently homogeneous state.

### D. Sandwich-type LC cells

This mixture of 5CB + MWCNT was introduced into a sandwich-type LC cell with  $20 \mu\text{m}$  thicknesses [5] called sometimes "the flat capillary" [12]. Polyimide alignment

layers were unidirectional rubbed for arrangement of the planar 5CB host texture [3]. The transverse electric field could be applied to LC cell for investigation of electrooptical effects including the Fredericksz transition of the composite to the homeotropic orientation of 5CB host.

### E. Optical investigations

Optical structures of nanocomposites were investigated and documented by modern optical polarization microscope Olympus BX51 with colour high-resolution CCD camera and computer controlled oven [13]. It allowed us to investigate the structure of 5CB + MWCNT composites in crystal, LC and isotropic liquid phases. The combined microscope objectives had prolonged focal length. Their precise movement along the microscope axis ( $\Delta z = 1 \mu\text{m}$ ) allowed study of the optical polarization structures, including topological structures around and between the aggregates of nanocomposites inside the LC cell in various cross-sections [4-7]. The scattering of propagating laser beams was investigated using a separate setup equipped by a He-Ne laser generating the lower transverse mode, i. e. Gaussian beams.

### F. Electrical conductivity measurements

The electrical conductivity measurements were done by Instek 819 under the external voltage of 0.2 V and frequency of 10 kHz applied to unaligned samples in a thick cell ( $\approx 0.5$  mm) in the temperature range of 293-350 K (at 2 K/min scanning rate both for heating and cooling). Each measurement was repeated, at least, 3 times for calculation of the mean values of experimental data.

## III. RESULTS AND DISCUSSIONS

### A. Spontaneous self-aggregation and percolation threshold

Freshly prepared 5CB+MWCNT composites undergo complicated incubation processes comprehensively investigated recently by a set of physical methods [6, 14]. The initial sonication resulted in homogeneous dispersing of MWCNTs; however, after short period of time a large quantity of spatially distributed aggregates were formed. The transformation of homogeneous distribution of MWCNTs into the segregated state is believed to occur owing to the aggregation between different nanotubes. The efficiency of aggregation is controlled by (i) strong and highly anisotropic van der Waals interactions [1, 2] and (ii) Brownian diffusion of individual nanotubes.

The simple Smoluchowski approach was applied to estimation of the half-time of aggregation. In this approach, the MWCNTs were modelled by cylindrical par-

ticles with huge aspect ratio  $r = l/d$  ( $r \gg 1$ ), where  $l$  is the length and  $d$  is diameter of MWCNT. Under assumption that cylindrical particles can aggregate when the distance between them is of the order of their length  $l$ , the half-time of aggregation  $\theta$  can be estimated as

$$\theta = (4D\pi nl)^{-1}, \quad (1)$$

where  $D$  is the diffusion coefficient and  $n$  is the numerical concentration of the particles. These values can be estimated as

$$D = kT \ln r / (3\pi\eta rd) \quad (2)$$

and

$$n = (\rho/\rho)C/V, \quad (3)$$

respectively, where  $kT$  is the thermal energy,  $\eta$  is viscosity,  $\rho/\rho$  is the ratio of densities of 5CB and MWCNTs ( $\rho/\rho \approx 0.5$ ),  $C$  is the mass fraction of MWCNTs in 5CB, and  $V_c = \pi d^3 r / 4$  is the volume of a single MWCNT.

Finally, the following relation can be obtained:

$$\theta \approx 3\pi d^3 \eta / (8kTC)(r / \ln r). \quad (4)$$

Taking into account that  $\eta \approx 0.1 \text{ Pa}\cdot\text{s}$  (viscosity of 5CB),  $d = 20 \text{ nm}$ ,  $r = 500$ ,  $T = 300 \text{ K}$  (temperature), we obtain  $\theta \approx 180 \text{ s}$  at  $C = 0.01 \text{ \% wt}$  and  $\theta \approx 18 \text{ s}$  at  $C = 0.1 \text{ \% wt}$ .

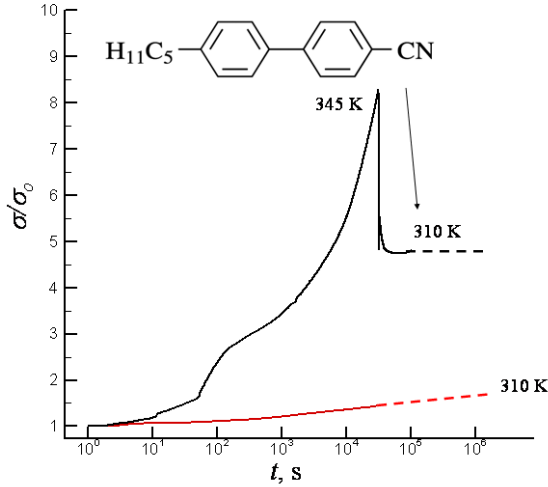


FIG. 1: Time dependencies of the relative electrical conductivity  $\sigma/\sigma_o$  ( $\sigma_o$  is initial electrical conductivity) in 5CB+*o*-MWCNTs composites (0.1 % wt) incubated at 310 and 345 K. The decrease of  $\sigma/\sigma_o$  in a sample incubated at  $T=345 \text{ K}$  during its cooling to 310 K reflects the temperature effect on  $\sigma$ .

The detailed investigations have shown that the structure of nanocomposites and their physical characteristics attain stable values only after several hours or days after sonication. It can be explained by existence of the mechanism causing compacting of the ramified, or loose, aggregates (*L*-aggregates) formed in the "fresh" suspension into the more compacted aggregates (*C*-aggregate)

formed in thermally incubated composite samples. These structural changes were confirmed by the presence of changes in electrical conductivity, which evidently reflects changes in the microstructure of samples during the transformation of *L*-aggregates to *C*-aggregates (Fig.1). The relative conductivity  $\sigma/\sigma_o$  ( $\sigma_o$  is the initial conductivity of the system after sonication) increased with time, however, the observed effects were more pronounced at high temperatures.

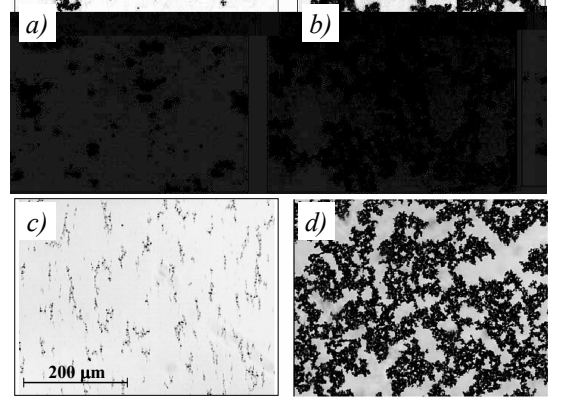


FIG. 2: Spontaneously self-aggregated clusters of "long" (*o*-MWCNT) (a, b) and "short" (*m*-MWCNT) (c, d) at various concentrations of MWCNTs: a, c - onset of aggregation (0.0025 and 0.005 wt %), b, d - percolation (0.025 and 0.25 wt %).

The several (5-7) day incubation at room temperature resulted in stabilization of microstructure, optical and electrical conductivity characteristics, and our experimental data presented below were obtained just for such stable samples. Note that formation of *C*-aggregates with irregular ramified borders [10] was visually observed by optical microscopy investigations even at rather low concentrations of MWCNTs (0.01-0.1 % wt). Such behaviour was observed both for "long" (*o*-MWCNTs) and "short" (*m*-MWCNTs) nanotubes (Fig.2). In both cases, the structural transformations were similar: from small islands (Fig.2a, c) up to the percolation structure with neighbouring clusters touching each other as their dimensions increase with concentration of nanotubes (Fig.2b, d).

The cluster transverse dimensions start from few microns. Their system expands over the whole LC cell when percolation structure is reached. At this moment, the nematic 5CB host is broken into a system of isolated "lakes" in 2D and sinuous "channels" in 3D. Moreover, formation of the percolation structure is accompanied by a drastic increase of electrical conductivity by 1-2 orders of magnitude [4, 6, and 10]. It was observed that unmodified nanotubes (*o*-MWCNTs) were forming the percolation networks at  $C = C_p \approx 0.025 - 0.05 \text{ \% wt.}$ , whereas the modified nanotubes (*m*-MWCNTs) were forming the percolation networks at  $C = C_p \approx 0.25 \text{ \% wt.}$  So, the percolation threshold concentration was 5-10 time higher for

*m*-MWNTs than for *o*-MWNTs. Extremely small percolation threshold concentrations are rather typical for such composites and can be explained by the high aspect ratio ( $r \approx 100-1000$ ) of MWCNTs. Increase of the percolation threshold for modified nanotubes (*m*-MWCNTs) ( $C = C_p \approx 0.1-0.25\%$  wt.) possibly reflected the shorter length and smaller aspect ratio  $r$  of the modified nanotubes.

### B. Theoretical model of fractal aggregation of MWCNTs in the nematic LC matrix: formation of *L*-aggregates

The above-described formation of nanotube aggregates in the nematic LC matrix can be better understood using the following theoretical model. The MWCNTs of *L*-aggregates can be considered as linear elements forming a compact skeleton of a certain regular surface that bounds a certain confined space. We determine the volume encompassed by the skeleton considering only one characteristic spatial dimension of MWCNT- its linear length  $l$ , which is fully justified if the aspect ratio  $r \gg 1$  ( $r = l/d$ , where  $d$  is the characteristic lateral dimension (diameter of MWCNT)).

From geometrical similarity considerations, the volume of a cluster with characteristic linear dimension  $l$  can be presented as

$$V_{cl} = V_{cl}(l) = A_{cl}l^3, \quad (5)$$

where  $A_{cl}$  is a constant depending on the cluster geometry (e.g.,  $A_{cl} = 1$  for cubic spatial structure,  $A_{cl} = \sqrt{2}/12$  for spatial structure formed by tetrahedrons, etc.). Similarly, the total volume of the nanotubes comprising the skeleton is  $V_{nt}(l) = lB_{nt}g(d)$ , where  $B_{nt}$  is another constant. The value of  $B_{nt}$  depends upon cluster geometry accounting for the number of nanotube edges comprising one cell of the skeleton. Function  $g(\dots)$  determines the volume of a single nanotube in the cluster as a function of its characteristic cross-section area. The form of  $g(\dots)$  in the case of a regular skeleton depends upon geometry of isolated nanotubes accounting for the bends, fractures, deviations from cylindrical shape, scatter of lateral dimensions, etc. In the case of fractal geometry,  $g(\dots)$  should "feel" how the nanotubes are connected and should depend on the fractal "coastline" picture in the direction normal to their predominant orientation. In a general case

$$g_f(x) \sim x^{d_f}, \quad (6)$$

where  $d_f$  is the fractal dimension of the cluster and for regular geometry  $d_f = 2$ .

For regular skeleton geometry, the total volume of nanotubes in the skeleton is

$$V_{nt}(l) = lB_{nt}g(d). \quad (7)$$

If nanotubes are cylindrical,

$$g(d) = (\pi/4)d^2 \quad (8)$$

and

$$V_{nt} = B_{nt}l^3r_{-2} \quad (9)$$

in terms of the nanotube length and aspect ratio. It can be verified that  $B_{nt} = 3\pi/2$  for tetrahedral skeleton cells;  $B_{nt} = 3\pi$  for cubic cells, etc...

Thus, the volume ratio of the cluster and the regular skeleton (i.e., the ratio of the volume encompassed by the nanotube skeleton and the total volume of the nanotubes involved) is

$$W_a = V_{cl}/V_{nt} = (A_{cl}/B_{nt})r^2 = Ar^2. \quad (10)$$

With increase of aspect ratio  $r$  (i.e., when nanotubes become longer or thinner),  $W_a$  grows rapidly, while the volume with nematic molecules "captured" by the nanotube skeleton (the volume of the "coat") increases much slower (not faster than linearly). The coefficient  $A$  depends on the specific skeleton geometry, and its value can vary within  $10^{-1} > A > 10^{-2}$  ( $= 1/3\pi \approx 0.1$  for cubic cells,  $\approx 0.025$  for tetrahedral cells).

Thus,  $W_a$  is the ratio of the *L*-aggregate volume (i.e., the volume of a loose skeleton formed by the nanotubes together with "captured" molecules of the dispersion medium (nematic LC) both "inside" the skeleton and in the nearest coordination layers) to the total volume of nanotubes comprising the skeleton. If  $C = V_{nt}/V$  is the volume fraction (or mass fraction if the difference between the densities of the dispersion medium and nanotubes can be neglected) of nanotubes that were introduced into the matrix, the value of  $C_a = cW_a$  can be considered as effective volume concentration of *L*-aggregates in the matrix (solvent, dispersion medium).

In the case of fractal geometry, both the surface of the skeleton formed by the nanotubes and the outer surface of *L*-aggregate formed by the aggregated nanotubes and captured molecules of dispersion phase will be of fractal character. Accounting for the fact that *L*-aggregates are formed in orientationally ordered matrix by orientationally ordered nanotubes, it is reasonable to expect that these aggregates should be essentially oblate (flattened). It leads us to a heuristic formula

$$W_a = V_{cl}/V_{nt}. \quad (11)$$

Correspondingly, the effective concentration of aggregates in the LC+MWCNT dispersion is

$$C_a = CW_a = Cr^{d_f}A_{cl}/B_{nt} = CAr^{d_f}. \quad (12)$$

Thus, the effective concentration of *L*-aggregates at a given initial concentration of nanotubes appears to be a universal function of the aspect ratio, which is rather

attractive. The proportionality coefficient depends on specific geometry of the nanotubes and the fractal skeleton structure formed by them; it can be considered as constant for a given type of the nanotube dispersions. As it was noted above, its value can be taken as falling within 0.025 - 0.1.

This formula accounts at semi-empirical level for all main factors affecting aggregation of the nanotubes: the initial concentration of nanotubes  $C$ , their aspect ratio  $r$ , geometry of cluster formation  $A$  and fractal dimensionality of the formed aggregates  $d_f$ . This formula can be easily verified experimentally. Thus, for two different MWCNT+LC dispersions prepared and studied under the same conditions but differing by certain parameters (e.g., aspect ratio  $r$  and/or nanotube concentration  $C$ ), the other measured characteristics should be related by equation (2). Preliminary verification can be done using data from [13]. In this paper, Fig.3 shows values for three concentrations of the nanotubes (generally speaking, for three specific cases of  $L$ -aggregate formation). According to (1.3), at  $r = 100$  and  $A = 0.1$ , we obtain for  $C = 0.1$  % and  $d_f = 1.81$  the value of  $W_a = 417$ , i.e., the total volume of the formed  $L$ -aggregates with fractal dimensionality 1.81 will make  $C_a = 41.7$  % from to total volume of the system (the remaining 58.3 % is the volume occupied by orientationally ordered nematic molecules that remained "free", i.e., not captured by the aggregates). Accordingly, we get  $C_a = 12$  % for  $C = 0.01$  % and  $d_f = 1.54$ . This is in a semi-quantitative agreement with results of microscopic observations: the aggregates are relatively few and visually occupy  $\approx 10$  % of the visible area in dispersions with 0.01 % of MWCNTs, while in dispersions with 0.1 % of MWCNTs there is much more aggregates, their size is larger, and they occupy about one half of the visible area. A similar effect is experimentally observed when we do not increase concentration of the MWCNT, but changes occur with time in a freshly dispersed sample (incubation phenomena). After several hours the fraction of area occupied by the aggregates substantially increases ([13], Fig.6).

Behavior of 5CB molecules inside the aggregates and in the interfacial layers has features in common with the properties of nematic molecules inside micropores, which is also a challenging problem [19]. In this case, essential differences are also noted in molecular mobility and physical properties of the "bulk" and interfacially ordered portions of the nematic.

### C. Capturing of LC molecules inside skeleton and interfacial LC layers in the vicinity of aggregates

Analysis of the obtained data allows us to assume that formed aggregates consist of a nanotube skeleton and a large number of small 5CB molecules (sized 1.5.2.3 nm) captured inside this skeleton. It reflects the effect of extra-strong anchoring of 5CB to the side walls of MWCNTs. As a result, the average orientation of 5CB

molecules (nematic director) near the MWCNTs layers is perturbed due to random orientation of the nanotube axes with respect to the regular planar orientation of molecules in the 5CB host. Due to the strong interaction between the MWCNTs and neighbouring 5CB molecules, there appears a complex *interfacial layer* of LC molecules near the surface of aggregates. As a result, the MWCNT aggregates appear to be encapsulated by such interfacial layers.

These layers with strongly perturbed LC directors are anchored to the extremely ramified border of aggregate and extend to the bulk 5CB with unperturbed orientation of director. Formation of the interfacial layers leads to new optical properties of 5CB + MWCNT composites, resulting in creation of a new type of the complex light. Indeed, one of the fundamental properties of LCs is existence of elastic forces, which tend to orient the neighbouring molecules in parallel to director [3]. These forces are expected to be especially strong in the investigated composites due to extra large energy of 5CB molecule anchoring to the nanotube. It was shown that anchored 5CB molecules mostly retain their positions in any phase, including isotropic liquid [4]. Quite different is the structure of the outer part of the interfacial layer, which smoothly transfers into the structure of the unperturbed 5CB host and possesses microscale dimensions.

Strong elastic forces in the interfacial layers initiate development of heterogeneous LC structures both along the aggregate borders and in the transverse direction. This, in turn, induces random local birefringence in the interfacial layer, which manifests itself as bright spots on the dark background of unperturbed 5CB in the microscopic image of the aggregated composite observed through analyzer crossed to polarizer oriented along alignment layers of the LC cell host (Fig.3a). It was previously demonstrated that propagating laser beam gets scattered or diffracted on the interfacial layers, thus acquiring speckle-like structure full of optical vortices [4, 10]. Note that direct microscopic observations using high-quality polarization microscope [12] have confirmed existence of the microscale interfacial layers and have shown that mean thickness of such interfacial layers in 0.0025 wt % composite was 1  $\mu\text{m}$  [4]. Note that the size of 5CB molecules is only 1.5-2.3 nm, so, the interfacial layers may include thousands of monomolecular 5CB layers.

### D. Electrooptical investigation of interfacial LC layers in the vicinity of aggregates

The interesting responses of electrophysical properties to the transverse external electric field applied to a sandwich-type LC cell of thickness  $d$  were already observed [3 - 6]. The 5CB molecules are anchored strongly to the side walls of nanotubes and can retain their position upon application of the electric field. The birefringent structure of composites observed between the crossed polarizer and analyzer shows that the structure

of the interfacial layer, as well as its birefringence, drastically changes when the applied voltage  $U$  approaches the Fredericksz transition threshold (Fig.3).

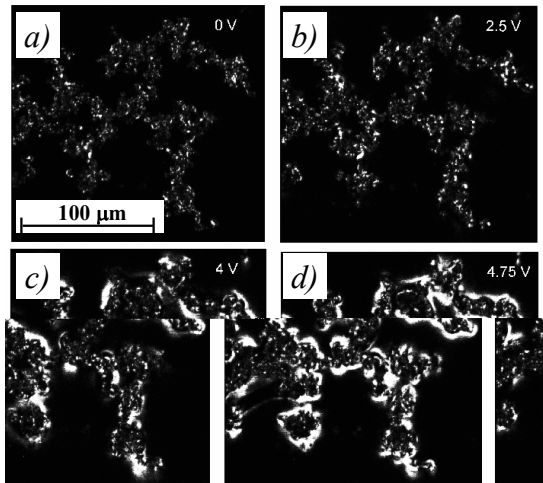


FIG. 3: Interfacial 5CB layer in the vicinity of the aggregates of nanotubes ( $\alpha$ -MWCNT, 0.005 wt %) as a function of the applied transverse electric field (analyzer A is crossed to polarizer P oriented along the rubbing direction of the alignment layers): a - without field,  $U = 0$ ; b -  $U = 2.5$  V; c -  $U = 4$  V; d -  $U = 4.75$  V. The scale of black-and-white brightness is given on the right.

New isolated bright spots appear at  $U = 2$  V when re-orientation of 5CB molecules to the homeotropic alignment begins (compare Fig.3a and Fig.3b). The mean thickness of interfacial layers in 0.0025 wt % composite increases from  $1 \mu\text{m}$  up to  $\approx 4.5 \mu\text{m}$  when nematic structure of 5CB undergoes the Fredericksz transition from planar to homeotropic orientation under the applied transverse electric field  $\approx 2.5$  V [4]. Above the Fredericksz threshold, a large portion of 5CB molecules in the interfacial layers turn from initial planar to homeotropic orientation, and the average thickness of the interfacial layer increases (Fig.2c, at  $U = 4$  V) and reaches its maximal value at  $U = 4.5$  V (Fig.3d).

However, the further electric field increase up to  $U \approx 6$  V decreases the layer thickness to  $\approx 2 \mu\text{m}$  [4]. Further increase of the applied field decreases the interfacial layer thickness because most of 5CB molecules on the outer border of the interfacial layer also re-orient to homeotropic arrangement. As a result, the visible thickness of the interfacial layers around the aggregates diminishes [4]. Note that detailed investigations have shown the presence of quite different responses to the applied field in the inner "lakes" and at the outer borders of MWCNT clusters. These differences may be explained by different degree of LC structure perturbation. The interfacial layers at the outer borders are less perturbed and there exist smooth transition from interfacial zone to unperturbed homeotropic state of 5CB.

#### E. Electric field induced formation of inversion walls (IW) between branches of MWCNT aggregates

Application of electric fields with voltage exceeding the Fredericksz transition provokes also formation of singular "channels" in the LC space between MWCNT aggregates. Figure 4 compares the microscopic images of the composite samples at  $U = 0$  V (a, b) and at  $U = 3.5$  V (c, d). The field-induced linear topological structures resemble those known as inversion walls, IWs [3, 16-20]. The IWs were first observed in a pure LC under the transverse magnetic field [3]. They were obtained later by laser irradiation of nematics in cells with small pre-tilt [20]. As in the previously mentioned cases, in our experiments the IWs were presented by three stripes, one bright central and two dark lateral ones, which were observed between parallel polarizer and analyzer: (Fig.4c, d).

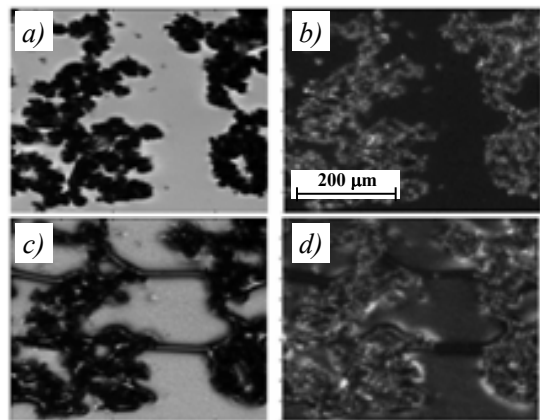


FIG. 4: Micro scale inverse walls in 5CB host between the neighbouring aggregates of long carbon nanotubes (0.01 wt %) induced by the applied transverse electric field. The microscope image of the actual aggregates is shown both without external field,  $U = 0$  V, (a, b) and under the applied field,  $U = 3.5$  V, (c, d). The polarizer and analyzer were parallel (a, c) and crossed (b, d).

Intensity distribution in IWs (Fig.5a) confirms that LC molecules of the central stripe remain mainly planar-oriented, unlike the auxiliary dark stripes with mainly homeotropic orientation of the director, which is in full accordance with the previously reported model (Fig.5b). Same as for IWs induced by magnetic fields in pure LC [3], the total width of IW diminishes with increase of the applied field (Fig.6). It can be speculated that spontaneous birth of IWs between aggregates of MWCNTs is initiated by the electric field-induced changes inside elastically strained overlapped interfacial layers formed between different aggregates. Formation of such IWs minimizes the internal stress in 5CB gaps between MWCNT aggregates. The formation of IWs reflects self-organisation in LC media that required free energy minimisation.

It was reported that IWs were produced on irregular borders of nematic layer in a LC cell [16, 19]. Evi-

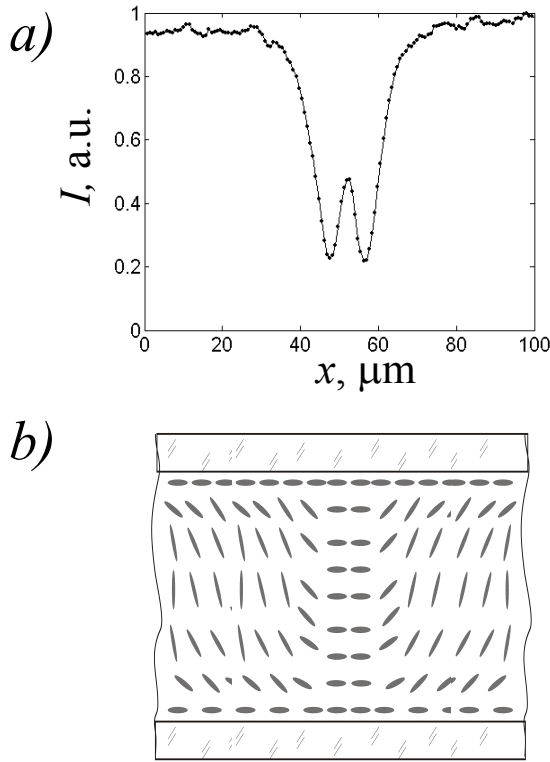


FIG. 5: Intensity distribution in the cross-section of induced inversion walls between the aggregates for parallel polarizer and analyzer (a). Schematic distribution of LC director in a cross-section of the inverse walls (b).

dently, the observed IWs were provoked by irregular fractal borders of MWCNT aggregates. Moreover, the IWs appeared only between some branches of the aggregates (Fig. 3). It seems reasonable to suggest that IWs appear between branches that induce splay and bend distortions of opposite sign (See [18], Fig.5c).

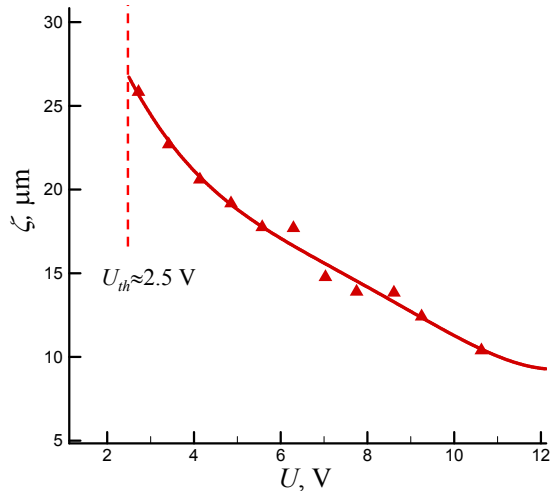


FIG. 6: Full width at half maximum  $\zeta$  of induced inversion walls versus the applied field voltage  $U$ .

Figure 6 presents the full band width at half maximum  $\zeta$  of IW versus the applied field voltage  $U$ . The value of  $\zeta$  was maximal at  $U = U_{th} \approx 2.5$  V and was decreasing with decrease of  $U$ . Typically, no noticeable dependence of  $\zeta$  upon the distance between different branches was observed.

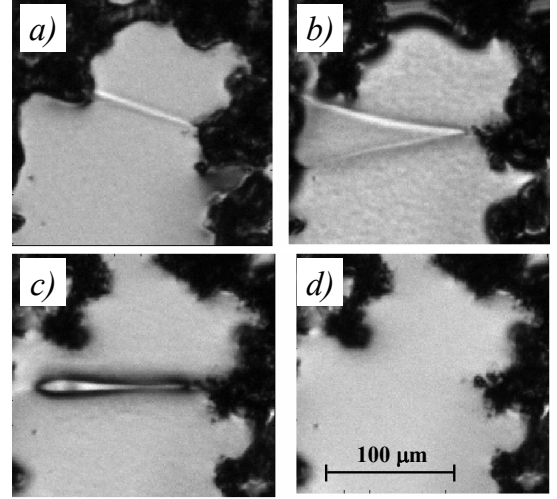


FIG. 7: Relaxation of the induced inversion walls when the applied electric field  $U = 9$  V (a) is turned off for different periods after turning the electric field off: 2s (b), 5s (c), and 7s (d).

Very elucidative is the transient evolution of the IW structure when the electric field is turned off (Fig.7a-d). As an example, in Fig. 7b (2s after turning electric field off), the left end of the "channel" splits in two different walls that move to the neighboring MWCNT branches. In Fig. 7c (5s after turning electric field off), IW has the form of a closed loop; the similar structure of IW was observed for pure LC under external magnetic field [3]. Finally, the system relaxes to the initial state in 7s after electric field is turned off. The observed effects were completely reproducible when the electric field was repeatedly turned on and turned off. This demonstrates that all the elastic strengths involved into formation of IWs obey the Hook law.

Finally, we noticed that formation of such IWs is related with some kind of self-organization minimizing elastic perturbations introduced by the nanotubes and the effects of IW formation and evolution in a LC composite system containing the nanotubes deserve more detailed consideration in future, both from experimental and theoretical points of view.

#### IV. CONCLUDING REMARKS

The main task of our investigations was to study the influence of carbon nanotubes on the micro and macro physical properties of their LC nanocomposites. Many properties of 5CB + MWCNT composites were thor-

oughly investigated by electrophysical methods. The major findings may be formulated as follows:

1. Spontaneous self-organization of the nanotubes producing the microscale aggregates in initially homogeneous dispersion was observed and investigated both theoretically and experimentally. The efficiency of aggregation is controlled by strong, long ranged and highly anisotropic van der Waals interactions and the Brownian diffusion of individual nanotubes. The simple Smoluchowski approach was used for estimation of the half-time of aggregation; it was shown that the process of aggregation includes the fast stage resulting in formation of loosed aggregates (*L*-aggregates) and the slow stage yielding compacted aggregates (*C*-aggregate). The aggregates have ramified fractal borders; formation of the percolation structures was observed at  $C = C_p \approx 0.025 - 0.05$  % wt for unmodified nanotubes (o-MWCNTs) and at  $C = C_p \approx 0.1 - 0.25$  % wt. for the modified nanotubes (*m*-MWCNTs).

2. The proposed theoretical model of *L*-aggregation is in good agreement with the experimental results. The microscale interfacial layer of host 5CB molecules substantially affects the optical and conductivity characteristics of the composites. Such layer is extremely heterogeneous both along the fractal borders and in cross-section. The inner borders of the layer are fixed to the side walls of individual nanotubes due to extra strong anchoring, in contrary to the outer borders, where orientation of director approaches smoothly its orientation in the un-

perturbed 5CB host.

3. Transverse electrical field application to a sandwich-type LC cell homeotropically orients the 5CB molecules, which leads to increase of elastic strengths in the interfacial layer, its thickness and induced birefringence. The inversion wall topological structures were observed for the first time in LC+CNT composites at threshold values of the applied field in the vicinity of Fredericksz transition. Cross-section structure of the inversion walls and their thinning with electrical field increase were the same as those observed earlier in pure nematic. The inversion walls were appearing between branches of some neighbouring MWCNT aggregates. Full relaxation of inversion walls was observed when the composite structure returned to its initial state after switching off the applied field. It witnesses that all the elastic strength changes obey the Hook law.

## V. ACKNOWLEDGEMENT

Authors are thankful to Profs. Yuri Reznikov and Victor Reshetnyak for useful consultations on LC physics, Dr. Vasil' Nazarenko for polarization microscope Olympus, computer controlled oven and useful LC discussions. This work was supported in part by Projects 2.16.1.4, 2.16.1.7, ISTCU Project 4687).

- 
- [1] Lagerwall, J. P. F., Scalia G. "Carbon nanotubes in liquid crystals". J. Mater. Chem. 18, 2890-2898 (2008).
  - [2] Rahman M., Lee W. "Scientific duo of carbon nanotubes and nematic liquid crystals", J. Phys. D: Appl. Phys., 42, (063001 (1-12) (2009).
  - [3] De Gennes, P., Prost, J., "The physics of liquid crystals", Clarendon Press, Oxford (1993).
  - [4] Ponevchinsky, V. V., Goncharuk, A. I., Vasil'ev, V. I., Lebovka, N. I., and Soskin, M. S., "Cluster self-organization of nanotubes in nematic phase: the percolation behaviour and appearance of optical singularities", JETP Lett. 91, 239-242 (2010).
  - [5] Ponevchinsky, V., Goncharuk, A. I., Lebovka, N. I., Soskin, M. S., "Optical singularities induced in a nematic-cell by carbon nanotubes", Proc. of SPIE Vol. 7613, 761306-1 (2010).
  - [6] Minenko, S.S., Lisetski, L.N., Goncharuk, A.I., Lebovka, N.I., Ponevchinsky, V.V., and Soskin M.S., "Aggregates of multiwalled carbon nanotubes in nematic liquid crystal dispersions: experimental evidence and a physical picture", Functional Materials, 17, No.4, 454-459 (2010).
  - [7] Lisetski, L. N., Minenko, S. S., Ponevchinsky, V. V., Soskin, M. S., Goncharuk, A. I., Lebovka, N. I., "Microstructure and incubation processes in composite liquid crystalline material (5CB) filled by multiwalled carbon nanotubes", Materials Science and Engineering Technology/ Materialwissenschaft und Werkstofftechnik, 42, p. xx-xx (2011) (accepted).
  - [8] Ponevchinsky, V. V., Goncharuk, A. I., Minenko, S. S., Lisetski, L. N., Lebovka, N. I., and Soskin, M. S. "Incubation Processes in Nematic 5CB + Multi-Walled Carbon Nanotubes Composites: Induced Optical Singularities and Inversion Walls, Percolation Phenomena", Nonlin. Optics, Quant. Optics (submitted).
  - [9] Feder, J., "Fractals" (Plenum press, New York, London, 1989).
  - [10] Park Kyung, Lee Seung, and Lee Young, "Anchoring a liquid crystal molecule on a single-walled carbon nanotube", J. Chem. Phys. C, 111, 1620-1624 (2007).
  - [11] Solomon, M. J., and Spicer, P. T., "Microstructural regimes of colloidal rod suspension sol, gel, and glasses", Soft Matter, 6, 1391-1400 (2010).
  - [12] Blinov, L. M., Katz, E. I., Sonin, A. A., Physics of thermotropic liquid crystals", Uspechi fizicheskikh nauk, 152, 449-477 (1987) (in Russian).
  - [13] <http://www.olympusamerica.com>
  - [14] Goncharuk A. I., Lebovka N. I., Lisetski L. N., Minenko S. S., "Aggregation, percolation and phase transitions in nematic liquid crystal EBBA doped with carbon nanotubes", J. Phys.D: Appl.Phys. 42, 165411-1-8 (2009).
  - [15] Frunza, L., Frunza, S., Kosslick, H., and Shoenhals, A., "Phase behaviour and molecular mobility of n-octacyanobiphenyl confined in molecular sieves: dependence on the pore size", Phys. Rev. E, 78, 051701 (2008).
  - [16] Helfrich, W., "Alignment-inversion walls in nematic liquid crystals in the presence of a magnetic field", Phys.

- Rev. Lett., 21, 1518-1521 (1968).
- [17] Demus., D., and Richter, L., "Textures in Liquid Crystals", Frelag Chemie, Weinheim, N. Y. (1978).
  - [18] Janossy, I., and Prasad, S. K., "Optical generation of inversion walls in nematic liquid crystals" Phys. Rev. E, 63, 041705 (2001).
  - [19] Figueiredo Neto, A. M., Marnitot-Lagarde, Ph., and Durand G., "Anisotropy induced director refraction inside inversion walls in nematic liquid crystals", J. Physique Lett, 45, L-793 - L-798 (1984).
  - [20] Cladis, P. E., van Saarloos, W., Finn, P. L., and Kortan, A. R., "Dynamics of Line defects in nematic liquid crystals" Phys. Rev. Lett., 58, 222-225 (1987).